Suppl. Figure 1 (Lee et al.,)

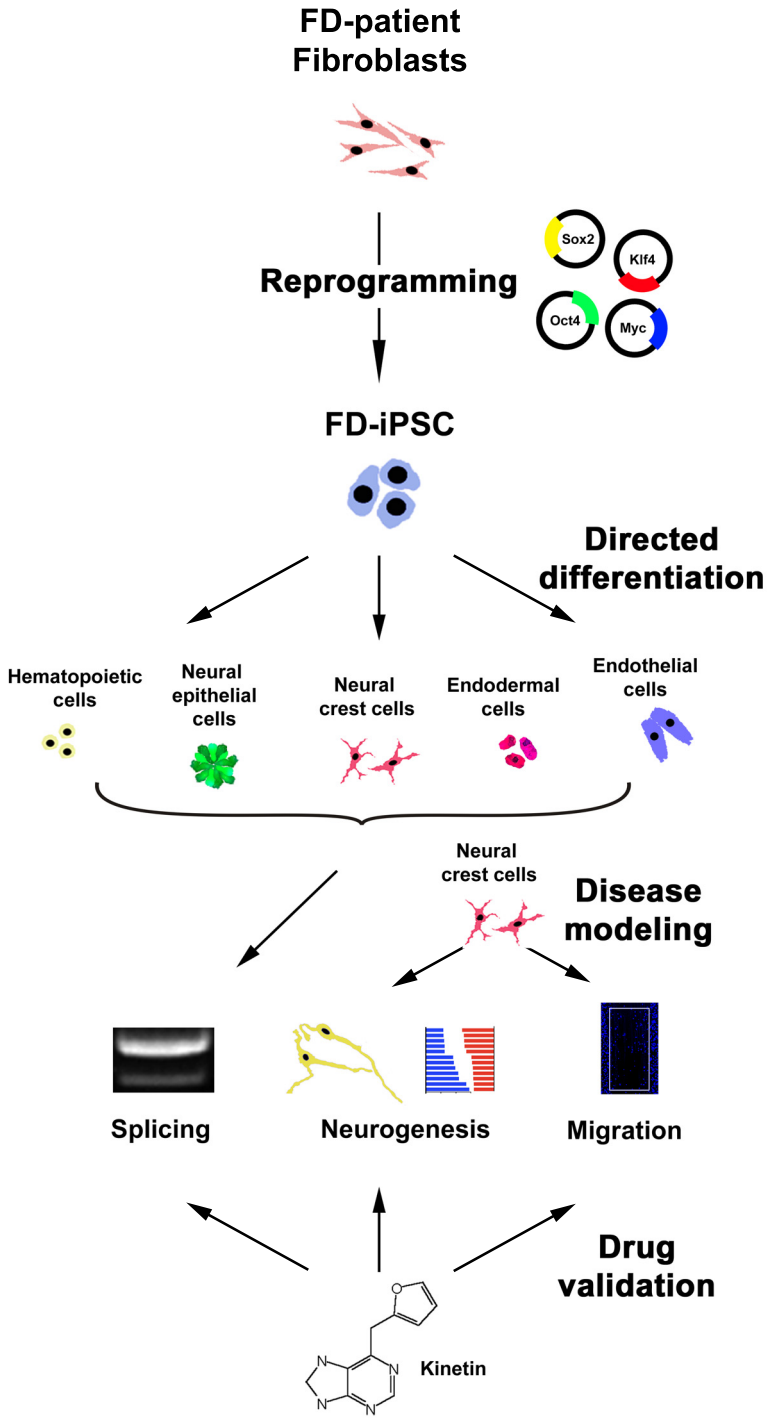

Suppl. Figure 2 (Lee et al.,)

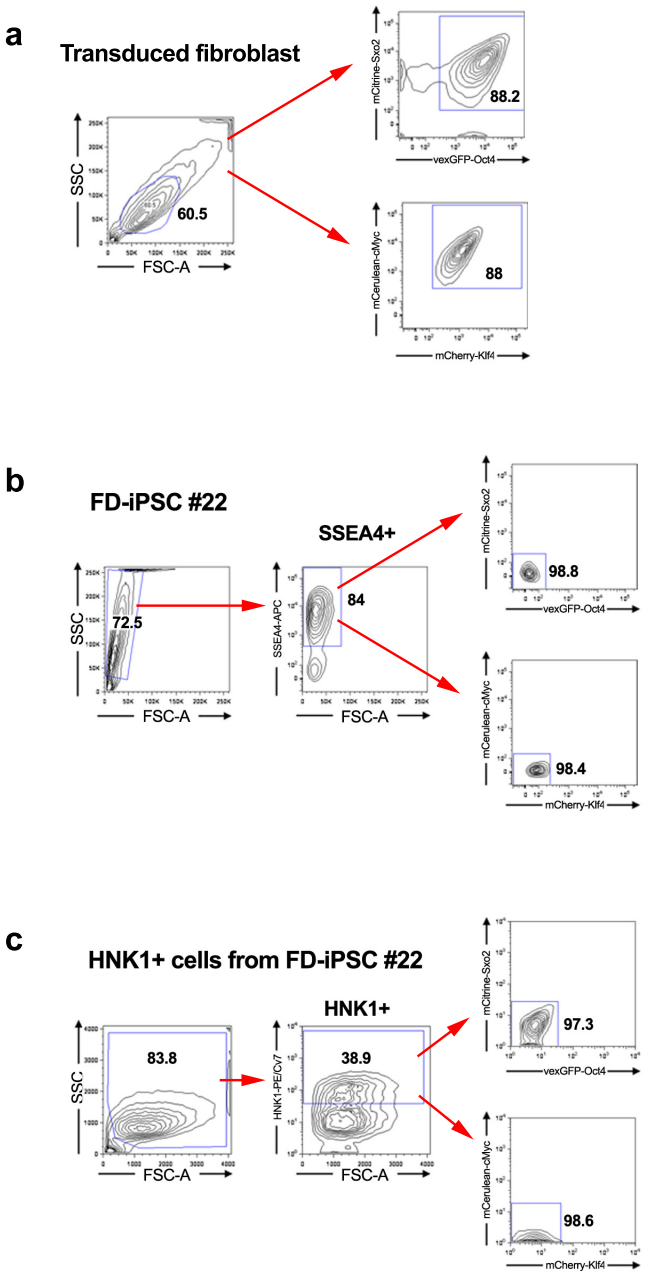

Suppl. Figure 3 (Lee et al.,)

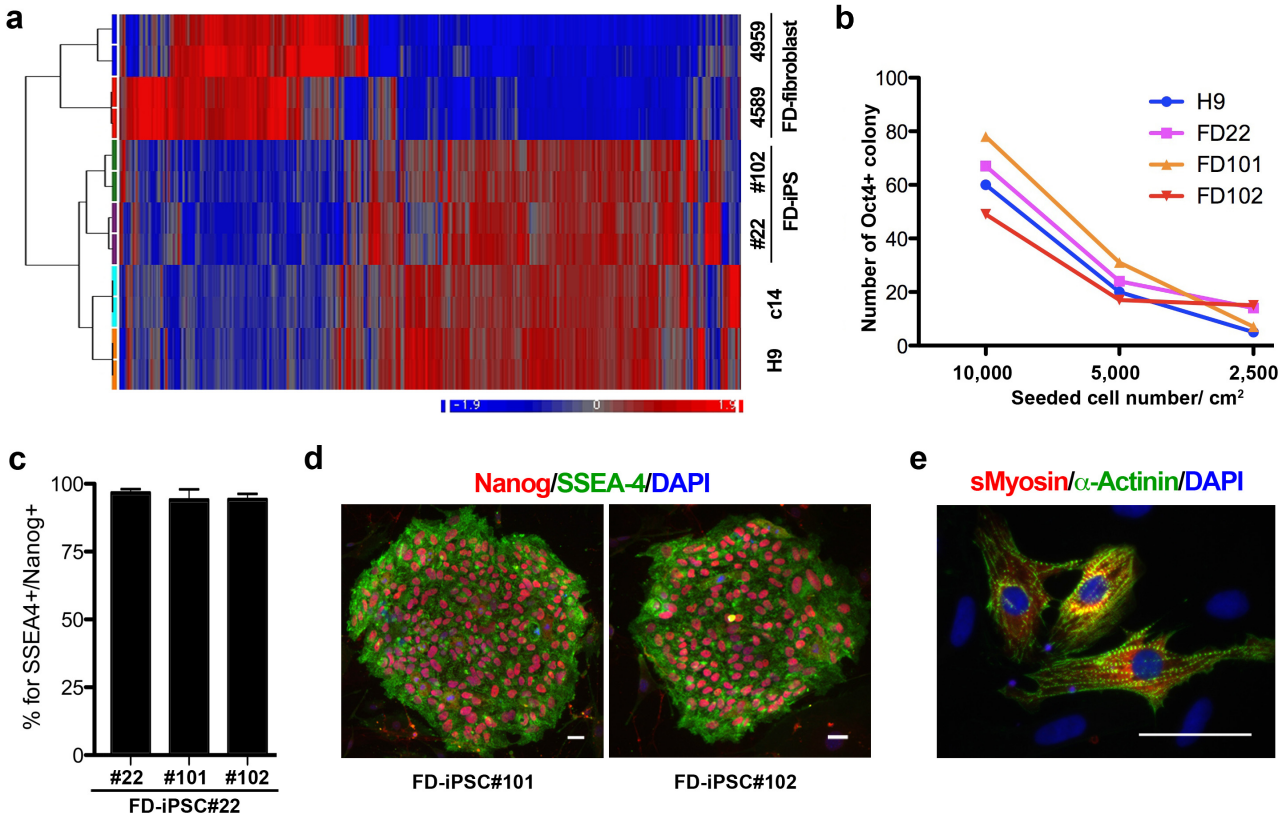

Suppl. Figure 4 (Lee et al.,)

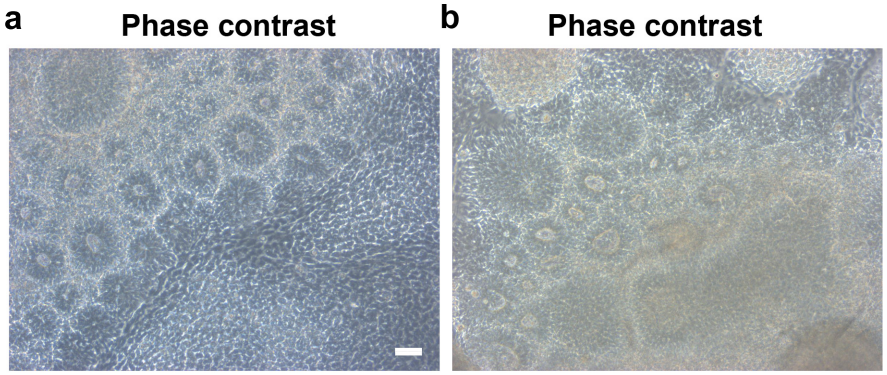

Suppl. Figure 5 (Lee et al.,)

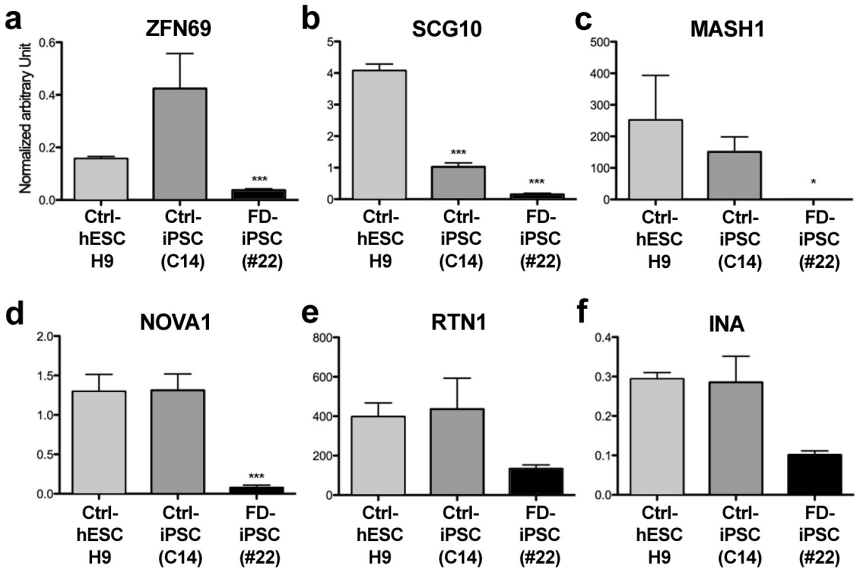

Suppl. Figure 6 (Lee et al.,)

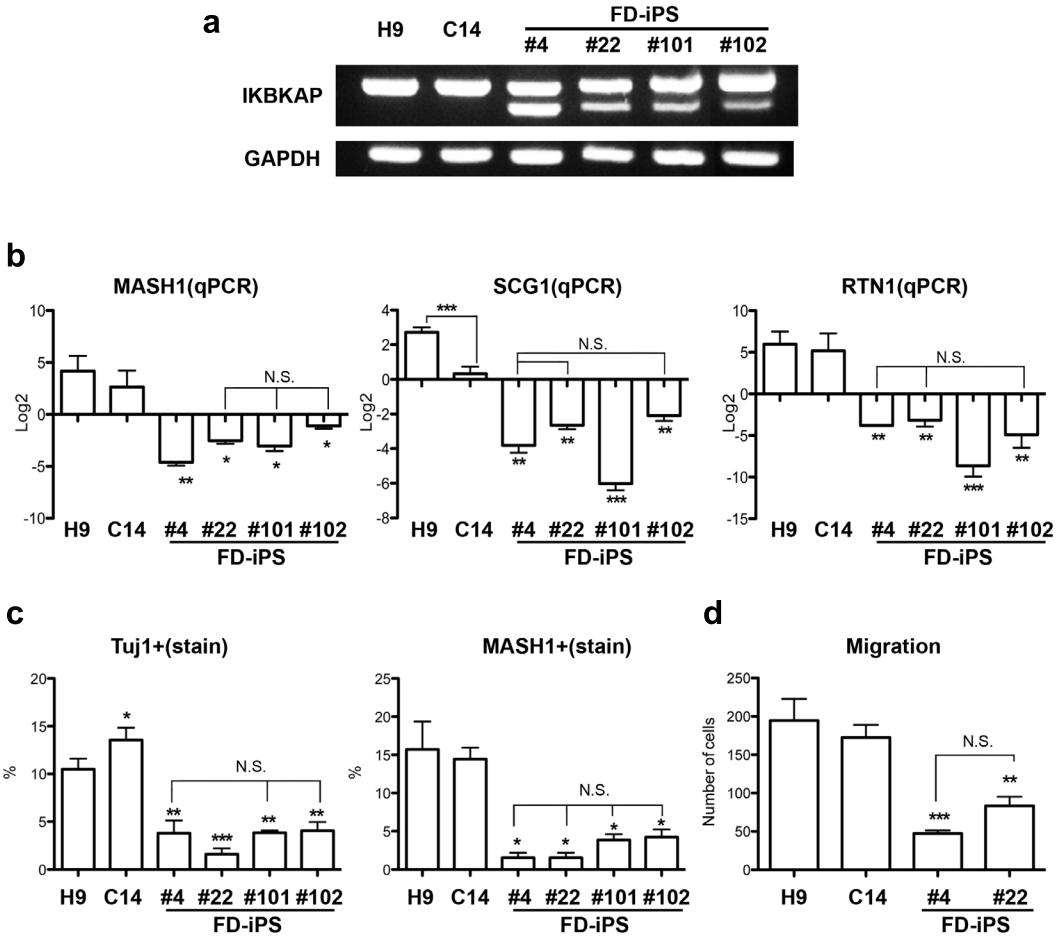

Suppl. Figure 7 (Lee et al.,)

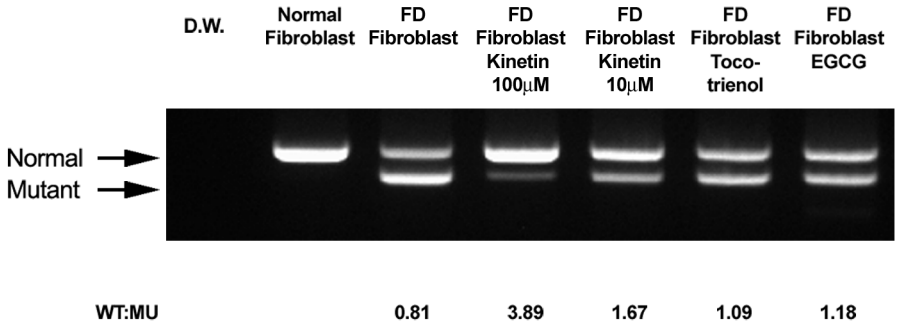

WT:MU		0.81	3.89	1.67	1.09	1.18

Suppl. Figure 8 (Lee et al.,)

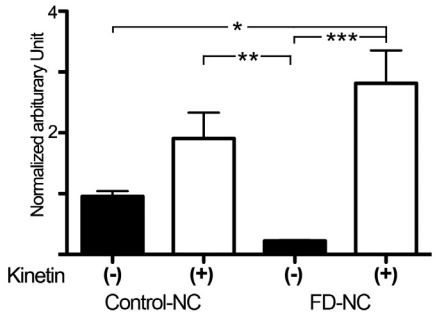

Suppl. Figure 9 (Lee et al.,)

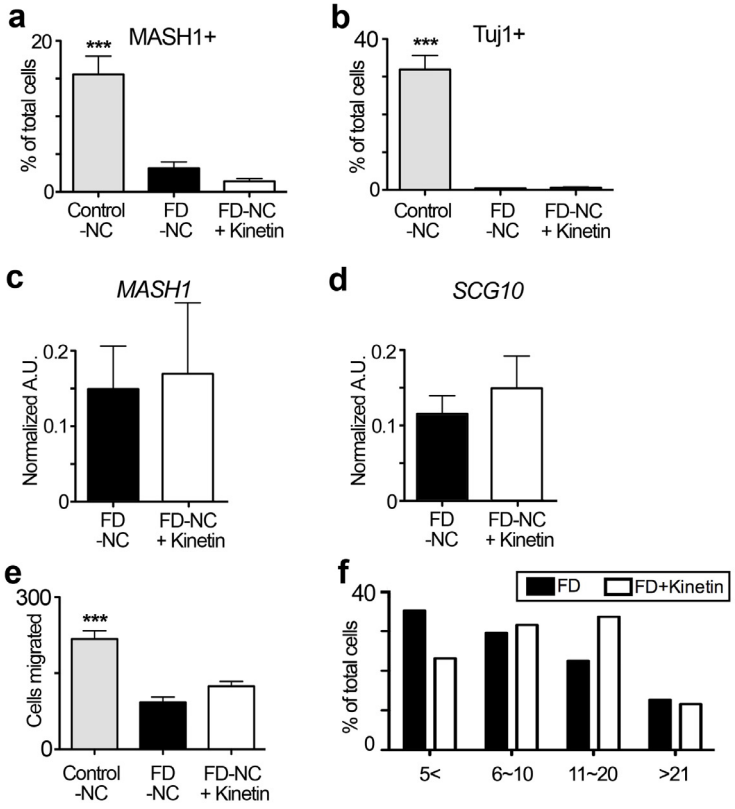

Suppl. Figure 10 (Lee et al.,)

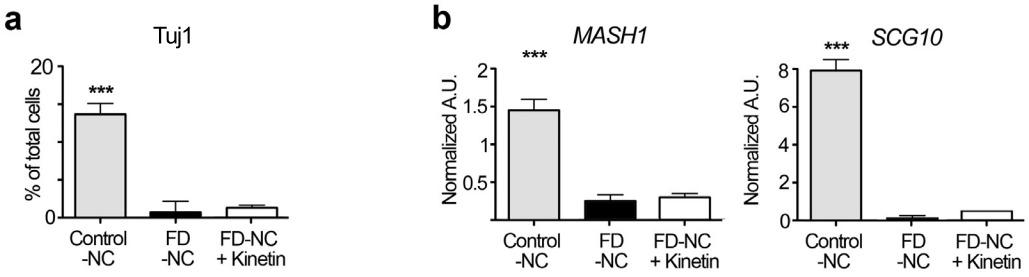

Suppl. Figure 11 (Lee et al.,)

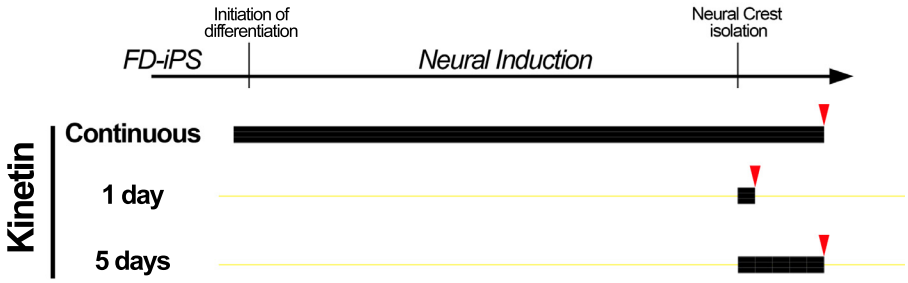

Supplementary Table 1 (Lee et al.,)

Marker	FD-fibroblast		FD-iPSC#22		FD-FD-iPSC#4	
Amelogenin	X		X		X	
CSF1PO	10	11	10	11	10	11
D13S317	11	12	11	12	11	12
D16S539	9	12	9	12	9	12
D18S51	12	14	12	14	12	14
D19S433	12	15	12	15	12	15
D21S11	28	29	28	29	28	29
D2S1338	19	23	19	23	19	23
D3S1358	14	18	14	18	14	18
D5S818	10	12	10	12	10	12
D7S820	9	11	9	11	9	11
D8S1179	13	16	13	16	13	16
FGA	20	22	20	22	20	22
TH01	9	9.3	9	9.3	9	9.3
TPOX	10	11	10	11	10	11
vWA	15		15		15	

DNA fingerprinting of FD-iPSC showed DNA characteristics of FD-fibroblasts.

Supplementary Table 2 (Lee et al.,)

Transcript	ILMN_Gene	Source_Reference_ID	logFC	P.Value
ILMN_4794	C21ORF81	NM_153750.1	2.884173408	1.57E-06
ILMN_18538	H19	NR_002196.1	2.683173843	8.96E-07
ILMN_22149	FLJ21986	NM_024913.3	2.196014735	7.38E-05
ILMN_180334	VWF	NM_000552.3	2.148790098	2.90E-05
ILMN_29279	FBLN2	NM_001998.2	1.955337897	1.70E-05
ILMN_164846	KIAA0644	NM_014817.3	1.8580555	8.46E-06
ILMN_169116	AFAP1L2	NM_001001936.1	1.809489839	1.16E-05
ILMN_163188	FIGF	NM_004469.2	1.659135983	4.31E-07
ILMN_89328	HS.389313	Hs.389313	1.619566677	0.00014895
ILMN_15736	IL13RA1	NM_001560.2	1.421286302	7.49E-07
ILMN_6495	TNFRSF11B	NM_002546.3	1.395579468	0.000118736
ILMN_27265	CHURC1	NM_145165.2	1.319049502	2.89E-05
ILMN_20259	PLP1	NM_199478.1	1.304739937	0.000153142
ILMN_307977	MORC4	NM_001085354.1	1.278624579	9.45E-05
ILMN_9206	CRYM	NM_001888.2	1.27301767	9.32E-05
ILMN_164531	ANKRD38	NM_181712.3	1.268192544	0.000215291
ILMN_12751	OAF	NM_178507.2	1.245942985	0.000183826
ILMN_3829	ACCS	NM_032592.2	1.242753727	4.45E-06
ILMN_6177	BMP4	NM_130851.1	1.214781214	9.37E-06
ILMN_25028	TF	NM_001063.2	1.173448362	4.01E-06
ILMN_27821	CLYBL	NM_206808.1	1.160927576	0.000300404
ILMN_17554	AMMECR1	NM_015365.2	1.145738141	1.18E-06
ILMN_23394	HPRT1	NM_000194.1	1.14085776	0.000142328
ILMN_9568	ASB9	NM_024087.1	1.129005008	2.72E-07
ILMN_9206	CRYM	NM_001888.2	1.117264	0.00011581
ILMN_169203	CP	NM_000096.2	1.114868946	5.38E-06
ILMN_26975	TYW3	NM_138467.1	1.077157196	1.79E-05
ILMN_5077	PIGA	NM_020473.2	1.077150524	2.71E-05
ILMN_18271	SULF2	NM_018837.2	1.052286338	9.23E-05
ILMN_165827	HDHD1A	NM_012080.3	1.039753973	4.92E-05
ILMN_32090	LOC644366	XM_932149.2	1.037078593	2.11E-05
ILMN_28362	WWC3	NM_015691.2	1.023915639	0.000146221
ILMN_15956	RDH10	NM_172037.2	1.016464442	1.79E-05
ILMN_22647	KLHL14	NM_020805.1	1.011945814	9.16E-05
ILMN_170030	DACT1	NM_001079520.1	1.0115147	7.85E-05
ILMN_8247	NHS	NM_198270.2	0.997469947	9.30E-05
ILMN_22146	PRDX4	NM_006406.1	0.992339772	2.72E-05
ILMN_30265	LEF1	NM_016269.2	0.98741625	7.91E-06
ILMN_166179	SIRPA	NM_001040023.1	0.987323268	1.65E-05
ILMN_19796	MPP1	NM_002436.2	0.97883542	3.69E-05
ILMN_182292	HEYL	NM_014571.3	0.971764912	0.000120107
ILMN_166444	STAG2	NM_001042750.1	0.970232869	2.57E-05
ILMN_163323	TPBG	NM_006670.3	0.960905245	0.000291825
ILMN_26072	NGFRAP1	NM_206917.1	0.957603275	0.000322568
ILMN_22194	HAS2	NM_005328.1	0.944399507	0.000280537

Supplementary Table 2 (Lee et al.,)

ILMN_164415	HAS2	XM_001128807.1	0.93840572	6.02E-05
ILMN_3010	WBP5	NM_001006612.1	0.920411226	0.000175809
ILMN_73496	HS.71947	Hs.71947	0.917546503	2.08E-05
ILMN_5029	CBS	NM_000071.1	0.913170628	1.67E-05
ILMN_5795	RAX	NM_013435.2	0.906463612	3.04E-05
ILMN_85013	HS.291319	Hs.291319	0.906289783	2.32E-05
ILMN_18271	SULF2	NM_018837.2	0.897743953	3.00E-05
ILMN_19027	PSMD10	NM_002814.2	0.888655839	3.43E-05
ILMN_20959	PCDH19	NM_020766.1	0.885838233	1.19E-05
ILMN_22027	SLC38A11	NM_173512.1	0.860141115	1.33E-05
ILMN_7975	FHL1	NM_001449.3	0.857598387	0.000161719
ILMN_176398	COL23A1	NM_173465.2	0.856824604	0.000225299
ILMN_12677	TCEAL8	NM_001006684.1	0.855293138	2.07E-06
ILMN_23068	SMARCA1	NM_003069.2	0.838378876	2.45E-05
ILMN_26730	LAMP2	NM_013995.1	0.838034666	3.73E-05
ILMN_9293	PDHA1	NM_000284.1	0.837072167	1.16E-05
ILMN_28481	ID2	NM_002166.4	0.830936556	0.000226611
ILMN_26857	AXIN2	NM_004655.2	0.816805575	7.73E-06
ILMN_22164	EIF1AX	NM_001412.3	0.805545406	1.85E-05
ILMN_10409	USMG5	NM_032747.2	0.803370001	3.39E-05
ILMN_163255	OCRL	NM_000276.3	0.796037809	4.26E-05
ILMN_37889	USP9X	NM_001039591.2	0.793629928	0.000260908
ILMN_19667	HTATSF1	NM_014500.3	0.793215684	5.96E-05
ILMN_19772	PDE5A	NM_001083.3	0.789485664	0.000273453
ILMN_1730	RAP2C	NM_021183.3	0.786792349	5.56E-06
ILMN_180156	CREB3L2	NM_194071.2	0.785504886	0.000163805
ILMN_74815	HS.104091	Hs.104091	0.774955229	1.07E-06
ILMN_13785	UTX	NM_021140.1	0.766985507	0.000290741
ILMN_23116	BEX1	NM_018476.3	0.762644144	6.59E-05
ILMN_20106	PGM1	NM_002633.2	0.760365507	2.34E-05
ILMN_22254	ARHGAP28	NM_001010000.1	0.747663989	0.00029084
ILMN_8725	RPGR	NM_001023582.1	0.733410555	0.000275051
ILMN_26490	NLGN4X	NM_020742.2	0.733132843	0.000321327
ILMN_20584	CDC7	NM_003503.2	0.727371538	0.000178866
ILMN_28618	RP2	NM_006915.1	0.715778613	0.000116116
ILMN_21750	C1GALT1C1	NM_152692.3	0.701170121	5.19E-05
ILMN_29762	CLEC1A	NM_016511.2	0.700781636	1.40E-05
ILMN_15237	IPO8	NM_006390.2	0.696485446	0.000192633
ILMN_18732	TMEM31	NM_182541.2	0.687915774	9.91E-05
ILMN_10088	OFD1	NM_003611.1	0.671580571	0.000177409
ILMN_17284	RAB9A	NM_004251.3	0.662475513	0.00015034
ILMN_26730	LAMP2	NM_013995.1	0.662264402	4.31E-05
ILMN_23417	PRPS2	NM_001039091.1	0.659686656	0.000192231
ILMN_15188	DOCK10	NM_014689.2	0.657730755	0.000205074
ILMN_19890	RPS4X	NM_001007.3	0.653681381	7.87E-05
ILMN_24186	LHX8	NM_001001933.1	0.647794808	0.000326443
ILMN_23657	MTR	NM_000254.1	0.646912901	3.61E-05
ILMN_170623	LOC642559	XR_016333.1	0.64012685	0.000145557
ILMN_22104	AIFM1	NM_145813.1	0.634321488	2.37E-05

Supplementary Table 2 (Lee et al.,)

ILMN_30026	MERTK	NM_006343.2	0.632919526	0.000302029
ILMN_24904	STARD8	NM_014725.2	0.629368615	0.000240782
ILMN_3319	LRIG1	NM_015541.2	0.620981665	0.000153504
ILMN_25519	ATG4A	NM_178270.1	0.620616295	8.60E-05
ILMN_25647	SLC25A5	NM_001152.1	0.620083744	7.77E-06
ILMN_169671	LOC286467	XR_015266.1	0.61799742	3.64E-05
ILMN_17171	WDR44	NM_019045.3	0.617232333	0.000112327
ILMN_131699	HS.579518	Hs.579518	0.604306342	4.45E-05
ILMN_1522	FANCB	NM_152633.2	0.587872974	5.91E-05
ILMN_11525	APOE	NM_000041.2	0.58557308	0.000231617
ILMN_175509	NET1	NM_001047160.1	0.584096975	2.18E-06
ILMN_166518	YAP1	NM_006106.2	0.556459087	2.90E-05
ILMN_18046	TWIST2	NM_057179.1	0.552554793	6.79E-06
ILMN_181875	RPS6KA3	NM_004586.2	0.548639506	0.000263203
ILMN_16069	EDN3	NM_207032.1	0.54104333	1.00E-05
ILMN_3567	ROR1	NM_005012.2	0.539583468	0.000287733
ILMN_19975	MIA	NM_006533.2	0.537253661	0.000282071
ILMN_171723	SMC2	NM_001042550.1	0.53185848	8.55E-05
ILMN_23479	IQSEC2	NM_015075.1	0.53009245	0.000147209
ILMN_177774	GPR126	NM_020455.4	0.526376828	0.000207223
ILMN_12432	DHRS3	NM_004753.4	0.525894258	3.94E-06
ILMN_25582	DEPDC1	NM_017779.3	0.498595489	0.000237899
ILMN_28002	ID1	NM_181353.1	0.497939255	0.000277894
ILMN_170277	POU5F1	NM_002701.4	0.484508506	7.66E-06
ILMN_169022	BMP2	NM_001200.2	0.479601899	2.89E-05
ILMN_181787	IKBKE	NM_014002.2	0.479477756	0.000193999
ILMN_22712	FAM122B	NM_145284.3	0.468291624	2.41E-06
ILMN_24569	PDXK	NM_003681.4	0.461893446	2.80E-06
ILMN_26705	SRPX	NM_006307.3	0.458070261	0.0001431
ILMN_27702	C8ORF13	NM_053279.1	0.453752189	1.08E-05
ILMN_20617	CA5B	NM_007220.3	0.450853468	1.26E-05
ILMN_42330	SLC45A4	XM_933796.2	0.448688479	0.00027581
ILMN_7487	FLJ31132	NM_001004355.1	0.44656077	0.000202479
ILMN_8440	GPRASP2	NM_001004051.1	0.438519885	8.11E-05
ILMN_18157	EMILIN1	NM_007046.1	0.434469609	7.15E-05
ILMN_29247	MSL3L1	NM_078628.1	0.431502822	0.000109569
ILMN_92871	HS.444855	Hs.444855	0.424172966	3.17E-05
ILMN_20235	SYNGR1	NM_145731.2	0.42313116	1.48E-05
ILMN_14307	SLC25A14	NM_003951.2	0.421913233	0.000158984
ILMN_18859	STX3	NM_004177.3	0.412478292	0.000137231
ILMN_103172	HS.537004	Hs.537004	0.409781484	0.000152344
ILMN_23251	ZNF662	NM_207404.2	0.401750516	5.16E-05
ILMN_18521	MID2	NM_052817.1	0.399179402	0.000260594
ILMN_956	ZNF75	NM_007131.2	0.397562592	0.000278883
ILMN_7177	HGD	NM_000187.1	0.390303393	0.000113639
ILMN_25738	TTYH2	NM_032646.5	0.385889219	0.000193798
ILMN_103797	HS.538259	Hs.538259	0.385058436	0.00027486
ILMN_161945	BCORL1	NM_021946.2	0.376136034	0.000117928
ILMN_14813	LDLRAP1	NM_015627.2	0.369663222	7.27E-05

Supplementary Table 2 (Lee et al.,)

ILMN_21688	MME	NM_000902.3	0.367565997	0.000277213
ILMN_23078	RPIA	NM_144563.2	0.367296775	7.81E-05
ILMN_931	GPR160	NM_014373.1	0.364640035	0.000205152
ILMN_27164	SEPP1	NM_005410.2	0.364417234	0.000222209
ILMN_22194	HAS2	NM_005328.1	0.35902335	0.000199264
ILMN_28399	NGFR	NM_002507.1	0.357734075	0.000112569
ILMN_22028	ARHGAP19	NM_032900.4	0.350878962	0.00023207
ILMN_26013	RAI2	NM_021785.2	0.34613041	0.000244523
ILMN_309219	C20ORF82	NM_080826.1	0.334799173	0.000283987
ILMN_45448	CTSF	NM_003793.3	0.331369106	0.00010391
ILMN_12434	RERG	NM_032918.1	0.322305768	4.01E-05
ILMN_307543	C14ORF130	NM_001100417.1	0.310926674	0.000307753
ILMN_41170	INF2	NM_001031714.3	0.295177226	6.93E-05
ILMN_10700	PGM5	NM_021965.3	0.294643365	1.72E-05
ILMN_74924	HS.105618	Hs.105618	0.292457512	0.000286041
ILMN_27828	BFSP1	NM_001195.2	0.288533421	0.000145854
ILMN_172286	HCCS	NM_005333.2	0.288364856	0.000162565
ILMN_7428	KLK6	NM_001012964.1	0.280116571	0.000279942
ILMN_28016	ATP6V1B1	NM_001692.3	0.277345326	4.26E-05
ILMN_80916	HS.187578	Hs.187578	0.265631766	0.000233236
ILMN_177952	RTKN	NM_033046.2	0.262087429	0.000202154
ILMN_28062	C1QTNF7	NM_031911.3	0.262058444	0.000206247
ILMN_28278	LPAR1	NM_057159.2	0.25981454	0.000197581
ILMN_41103	LOC652324	XM_941748.1	0.255901456	0.000128672
ILMN_182711	LOC401233	NM_001013680.1	0.249808399	0.00026882
ILMN_170187	CEP72	NM_018140.3	0.233232472	0.000113494
ILMN_21742	IL1RAP	NM_002182.2	0.232129804	0.000234182
ILMN_29986	PTGS2	NM_000963.1	0.222249286	0.00027951
ILMN_162028	LOC730952	XR_015744.1	0.221323891	0.000237112
ILMN_8341	PCGF5	NM_032373.3	0.191943226	0.000299171
ILMN_6269	SLC17A7	NM_020309.2	-0.225586962	0.000277297
ILMN_13088	C8ORF38	NM_152416.2	-0.237991248	0.000163978
ILMN_164195	BLOC1S2	NM_001001342.1	-0.239252109	0.000195439
ILMN_17821	THRA	NM_003250.4	-0.257115766	5.84E-05
ILMN_75788	HS.121667	Hs.121667	-0.260006165	0.000193671
ILMN_11647	BZRAP1	NM_004758.1	-0.262050903	0.000191244
ILMN_29440	VTCN1	NM_024626.2	-0.263750168	0.000230314
ILMN_25089	TESC	NM_017899.2	-0.264033668	9.14E-05
ILMN_13009	ACTR1A	NM_005736.2	-0.266546702	0.000200944
ILMN_21942	YPEL4	NM_145008.1	-0.281596541	0.000315452
ILMN_165656	UNCX	NM_001080461.1	-0.303518667	0.000107634
ILMN_23420	PIBF1	NM_006346.2	-0.306067635	0.000182041
ILMN_16451	COQ9	NM_020312.1	-0.313680845	0.000153811
ILMN_136283	HS.584102	Hs.584102	-0.314847887	0.00014731
ILMN_28640	ANKS1B	NM_181670.2	-0.338833336	0.000131157
ILMN_23436	NOVA2	NM_002516.1	-0.359414642	7.82E-05
ILMN_180846	MYH7	NM_000257.2	-0.36651898	5.33E-06
ILMN_177693	SMPD3	NM_018667.2	-0.370049068	0.000289529
ILMN_13405	RAP1GAP	NM_002885.1	-0.382359504	7.31E-05

Supplementary Table 2 (Lee et al.,)

ILMN_10774	RASSF2	NM_170774.1	-0.382574509	0.000150229
ILMN_12963	WBP2	NM_012478.3	-0.385086055	6.27E-05
ILMN_81208	HS.193406	Hs.193406	-0.394864392	0.000211454
ILMN_5981	FLJ20160	NM_017694.3	-0.403580966	6.73E-05
ILMN_40881	LOC340260	XM_941336.2	-0.404205624	0.000123533
ILMN_25826	SBK1	NM_001024401.2	-0.410234615	2.98E-05
ILMN_1335	C11ORF71	NM_019021.1	-0.411663934	0.000245345
ILMN_10231	AIM2	NM_004833.1	-0.423881294	0.000148182
ILMN_22211	SEMA4A	NM_022367.2	-0.433531972	0.000235236
ILMN_26493	HIST1H2AC	NM_003512.3	-0.43589655	7.78E-05
ILMN_25463	GNG8	NM_033258.1	-0.442470365	0.000115005
ILMN_166084	C22ORF9	NM_015264.1	-0.448798733	0.000139173
ILMN_306709	ZNF239	NM_001099283.1	-0.451881084	7.52E-05
ILMN_19930	TMEM14A	NM_014051.3	-0.45293401	2.17E-05
ILMN_162145	FNBP1L	NM_001024948.1	-0.470460653	1.09E-05
ILMN_23986	ZMYND10	NM_015896.2	-0.477463065	0.000108597
ILMN_29380	TIMM22	NM_013337.2	-0.490685362	0.000286436
ILMN_166861	LOC649095	XM_001131851.1	-0.49172818	6.97E-05
ILMN_178374	KIAA1409	NM_020818.3	-0.49568322	4.07E-06
ILMN_23493	PBX3	NM_006195.4	-0.500642008	0.000204678
ILMN_30680	LOC550112	XR_001037.1	-0.502558008	1.74E-05
ILMN_31415	LOC202134	XM_932143.1	-0.508668662	0.000169333
ILMN_3112	CCDC106	NM_013301.2	-0.534474791	8.24E-05
ILMN_165884	LOC728006	XM_001128698.1	-0.535781568	5.25E-05
ILMN_20458	PCSK2	NM_002594.2	-0.544634679	5.74E-05
ILMN_15020	CBFA2T3	NM_175931.1	-0.556092679	0.00022127
ILMN_8451	MXRA7	NM_001008529.1	-0.55738466	0.000131481
ILMN_14005	RPAIN	NM_001033002.2	-0.572691551	0.000178281
ILMN_110827	HS.552096	Hs.552096	-0.574061977	0.000280821
ILMN_13103	PAK7	NM_177990.1	-0.588898687	1.71E-05
ILMN_26814	LHX1	NM_005568.2	-0.5984156	0.000187767
ILMN_29852	AMY1B	NM_001008218.1	-0.613578049	7.68E-05
ILMN_21318	BHLHB5	NM_152414.3	-0.614052687	0.000179963
ILMN_96141	HS.486010	Hs.486010	-0.622521608	0.000220908
ILMN_96169	HS.486362	Hs.486362	-0.626533244	4.07E-05
ILMN_175562	APC2	NM_005883.2	-0.65054771	0.000218009
ILMN_29751	SVOP	NM_018711.2	-0.65094831	8.82E-06
ILMN_28176	CBLN1	NM_004352.1	-0.653246093	0.000165549
ILMN_23906	MTMR7	NM_004686.3	-0.653722121	0.00021425
ILMN_21527	BRUNOL6	NM_052840.3	-0.657681074	6.16E-06
ILMN_24740	TACC2	NM_206860.1	-0.661566344	0.000271149
ILMN_10036	PCBP4	NM_020418.2	-0.665597607	0.000130201
ILMN_18994	MICAL1	NM_022765.2	-0.676850615	0.000141202
ILMN_15964	DLG2	NM_001364.2	-0.685819382	8.67E-05
ILMN_171454	MGC24039	NM_144973.3	-0.688171842	8.27E-05
ILMN_308156	GOLSYN	NM_001099743.1	-0.6887051	1.56E-06
ILMN_71044	HS.8038	Hs.8038	-0.704900772	8.78E-06
ILMN_12935	CAMKK2	NM_153500.1	-0.708546037	0.000120733
ILMN_14016	MAST1	NM_014975.1	-0.721532367	0.000101616

Supplementary Table 2 (Lee et al.,)

ILMN_73404	HS.66187	Hs.66187	-0.739461635	3.43E-05
ILMN_102651	HS.534913	Hs.534913	-0.768671182	0.000254614
ILMN_7661	CRMP1	NM_001313.3	-0.774916938	0.000241965
ILMN_28349	SLC37A1	NM_018964.3	-0.795797406	0.000190282
ILMN_5664	TERF2IP	NM_018975.2	-0.802392858	1.30E-05
ILMN_14516	RNF165	NM_152470.2	-0.806229535	2.91E-05
ILMN_19021	CADPS	NM_003716.2	-0.838561327	9.16E-06
ILMN_28602	SHISA2	NM_001007538.1	-0.844574981	0.000270268
ILMN_4854	HES6	NM_018645.3	-0.847373664	4.10E-05
ILMN_139392	ZNF491	NM_152356.2	-0.856278144	0.000137582
ILMN_9517	ATP6V0E2	NM_145230.2	-0.858623898	5.40E-05
ILMN_2195	SPG3A	NM_015915.3	-0.861608172	1.11E-05
ILMN_8955	NRCAM	NM_005010.3	-0.862128693	2.72E-06
ILMN_15951	NOVA1	NM_002515.2	-0.87199304	8.51E-06
ILMN_28536	RUNDC3B	NM_138290.1	-0.883186646	0.000144139
ILMN_20684	TSPAN7	NM_004615.2	-0.883388624	0.00013353
ILMN_30166	ST18	NM_014682.1	-0.884005424	0.000192362
ILMN_22353	KIF3C	NM_002254.6	-0.896488643	4.20E-05
ILMN_4065	3-Sep	NM_019106.4	-0.90582207	5.11E-05
ILMN_5524	FAM36A	NM_198076.4	-0.931036339	2.94E-05
ILMN_13498	FABP7	NM_001446.3	-0.940826772	7.74E-05
ILMN_14582	ARHGEF7	NM_145735.1	-0.967906331	0.000261185
ILMN_35173	LMTK3	XM_936372.2	-0.973555875	0.000211626
ILMN_30217	KCTD10	NM_031954.3	-1.002404439	1.72E-05
ILMN_4065	3-Sep	NM_019106.4	-1.010545504	5.51E-05
ILMN_15828	PGM2L1	NM_173582.3	-1.018131469	0.000283528
ILMN_171526	MAP6	NM_207577.1	-1.018456284	9.43E-05
ILMN_45961	LOC283683	XM_931224.1	-1.018872982	9.18E-06
ILMN_14093	SYT1	NM_005639.1	-1.024509741	7.35E-05
ILMN_30286	LOC387856	NM_001013635.2	-1.030101103	7.91E-05
ILMN_38941	5-Sep	NM_002688.4	-1.053259827	0.000195416
ILMN_15722	NOVA1	NM_006491.2	-1.054210868	7.64E-05
ILMN_177099	RAB6B	NM_016577.3	-1.063077917	0.000274542
ILMN_29470	RFTN1	NM_015150.1	-1.071849571	9.64E-05
ILMN_4868	CDK5R1	NM_003885.2	-1.098687775	0.00016337
ILMN_11325	CCNA1	NM_003914.2	-1.099551549	4.03E-07
ILMN_163847	TBR1	NM_006593.2	-1.110163743	0.000122049
ILMN_9016	RUNDC3A	NM_006695.3	-1.110188832	0.000316897
ILMN_18430	DCLK1	NM_004734.2	-1.119236848	5.13E-05
ILMN_7302	TAGLN3	NM_001008273.1	-1.124128508	5.17E-05
ILMN_22045	PHYHIPL	NM_032439.1	-1.12739938	9.70E-05
ILMN_178729	FSTL5	NM_020116.2	-1.143639898	0.000101416
ILMN_17259	NLRP2	NM_017852.2	-1.167234036	0.000215993
ILMN_86876	HS.347185	Hs.347185	-1.169750612	0.000177511
ILMN_7211	CRMP1	NM_001014809.1	-1.172423646	0.000302092
ILMN_22617	KIF1A	NM_004321.4	-1.174345091	3.44E-05
ILMN_17827	SCG2	NM_003469.3	-1.193019265	0.000224568
ILMN_82312	HS.212483	Hs.212483	-1.196158677	1.70E-05
ILMN_10344	POU2F2	NM_002698.2	-1.324022582	2.03E-06

Supplementary Table 2 (Lee et al.,)

ILMN_22638	NPTX2	NM_002523.1	-1.378885442	3.18E-05
ILMN_16399	TUBB3	NM_006086.2	-1.411074462	7.60E-05
ILMN_30021	SNAP25	NM_130811.1	-1.430828644	0.000251042
ILMN_166209	KIAA0363	XM_001133202.1	-1.431999403	0.00027131
ILMN_22293	KLC1	NM_005552.4	-1.494765099	0.000222789
ILMN_23656	SH3GL2	NM_003026.1	-1.495619849	3.68E-05
ILMN_178294	PCSK1	NM_000439.3	-1.5086561	6.45E-05
ILMN_110584	HS.551307	Hs.551307	-1.53342931	0.000143359
ILMN_22819	CNR1	NM_016083.3	-1.542052306	1.95E-05
ILMN_8091	TNRC4	NM_007185.3	-1.546940936	7.70E-05
ILMN_1495	HMP19	NM_015980.3	-1.587779943	0.000250368
ILMN_18781	MAP4	NM_030885.2	-1.597548861	2.99E-05
ILMN_17528	MEIS2	NM_172315.1	-1.615814692	0.000111091
ILMN_22291	RUFY3	NM_014961.2	-1.680531997	1.94E-05
ILMN_15248	SNAP91	NM_014841.1	-1.726425948	4.23E-05
ILMN_3667	MYT1	NM_004535.2	-1.739650619	0.000193631
ILMN_173747	D4S234E	NM_001040101.1	-1.761335984	0.000170665
ILMN_19345	ISLR2	NM_020851.1	-1.802727747	0.000216025
ILMN_174587	RTN1	NM_021136.2	-1.840762118	6.52E-05
ILMN_167702	FLJ25404	XM_001134320.1	-1.911286839	4.19E-06
ILMN_3435	RTN1	NM_206852.1	-1.936634937	1.04E-05
ILMN_23892	ASCL1	NM_004316.2	-1.954576925	3.23E-06
ILMN_31184	FLJ33790	NM_001039548.1	-2.001193542	8.48E-06
ILMN_9766	INA	NM_032727.2	-2.118681428	2.06E-05
ILMN_162349	STMN4	NM_030795.2	-2.251357097	0.000105361
ILMN_10286	SLC17A6	NM_020346.1	-2.28086546	1.09E-05
ILMN_27672	STMN2	NM_007029.2	-2.301403735	6.16E-06
ILMN_23104	ZNF69	NM_021915.1	-2.434994226	1.12E-05

Supplementary Table 3 (Lee et al.,)

Name		Seqeunce (5'->3')	Anne aling temp.	Amplicon size (bps)
IKBKAP (RT-PCR)	Forward	CGGATTGTCACTGTTGTGC	60	393(normal) 391(mutant)
	Reverse	GACTGCTCTCATAGCATCGC		
IKBKAP (qRT-PCR)	Forward	GCAGCAATCATG TGTCCC	60	142
	Reverse	ACCAGGGCTCGATGATGA		
IKBKAP (Sequencing)	Forward	CCATAAGGCTCAAAGCGAAA	60	619
	Reverse	TGAGTGTCACGATTCTTTCTGC		
Nanog (Bisulfite seq.)	Forward	AGAGATAGGAGGGTAAGTT TTTTTT	58	250
	Reverse	ACTCCCACACAAACTAACTT TTATTC		

Supplementary Figures, Tables and Video

Supplementary Figure 1: **Schematic outline of study design.** FD-iPSCs were derived via reprogramming of patient specific fibroblast using a 4 factor protocol (Oct4, Sox2, Klf4 and Myc) in a lentiviral vector system. Following characterization of pluripotent state, FD-iPSCs were differentiated into multiple lineages (hematopoietic, neuroepithelial, neural crest, endothelial and endodermal cells) and purified based on surface marker expression. Differentiated lineages were used to demonstrate tissue specific *IKBKAP* splicing in FD-iPSC progeny. FD-iPSC derived neural crest precursors were further used to identify disease specific genetic and functional differences related to neurogenesis and cell migration. Drug validation studies assessed the potential of kinetin to mitigate disease-related effects on splicing, neurogenesis and migration in FD-iPSC derived neural crest precursors.

Supplementary Figure 2: **Silencing of 4 factors during reprogramming and lack of reactivation upon differentiation. a,** Transduced fibroblasts were analyzed by flow cytometry to determine transduction efficiency. **b-c**, Representative flow cytometric analysis of FD-iPSCs (SSEA4+) and differentiated neural crest cells (HNK1+) showed lack of transgene expression based on fluorescence reporter signal.

Supplementary Figure 3: **Additional characterizations of pluripotency in FD-iPSC lines. a,** Heatmap analysis and hierarchical clustering showed that the global gene expression profiles of FD-iPS cells were similar to those of human ESCs. **b**, FD-iPS and human ESC clones showed comparable survival and expansion of single cells (subcloning efficiency) upon dissociation in accutase. **c**, Percentages of SSEA4+ / Nanog+ colonies in multiple FD-iPSC lines. **d**, Representative images of SSEA4+/Nanog+ colonies in FD-iPS clones. **e**, Beating cardiomyocytes (**Supplementary Video 1**) were stained with sarcomeric myosin (sMyosin) and α-actinin. Scale bars in (**d**) and (**e**) correspond to 50μm.

Supplementary Figure 4: **Morphology of neural differentiation of FD-iPSC derived cells.** Representative images of neural rosettes derived from FD-iPSC #22 clone (**a**) and #4 clone (**b**). Scale bar correspond to 50μm.

Supplementary Figure 5: **Validation of microarray data by qRT-PCR analysis.** qRT-PCR analysis for confirmation of expression array data in control hESC (H9), iPSC (C14) and FD-iPSC derived neural crest precursors. $n = 4$; *, $P < 0.05$; ***, $P < 0.001$. All values are mean ± s. d.

Supplementary Figure 6: **Reproducibility of disease-related phenotypes among neural crest precursors derived from different FD-iPSC lines. a**, *IKBKAP* RT-PCR analysis of neural crest cells derived from control hESC (H9), control iPSC (C14) and four different FD-iPSC clones. **b-d**, qRT-PCR analyses, quantification of Tuj1 and MASH1 protein expression and migration assay in neural crest cells derived from control hESC (H9), control iPSC (C14) and multiple FD-iPSC clones ($n = 3 - 6$; *, $P < 0.05$; **, $P < 0.01$; ***, $P < 0.001$. All values are mean ± s. d).

Supplementary Figure 7: **Gel image of IKBKAP RT-PCR upon treatment of FD fibroblasts with candidate chemical compounds.** The ratio of normal:mutant (WT:MU) splicing was significantly increased in kinetin treatment.

Supplementary Figure 8: **Quantification of normal IKBKAP transcript with kinetin treatment in control iPSC and FD-iPSC derived neural crest cell.** $n = 3$; *, $P < 0.05$; **, $P < 0.01$; ***, $P < 0.001$. All values are mean ± s. d.

Supplementary Figure 9: **Short-term (for 24 hours) treatment of kinetin for FD-iPSC derived neural crest cells. a-b**, Quantification of MASH1 and Tuj1 expressing neural crest cells derived from FD-iPSC with/without kinetin treatment and control-iPSC. MASH1 (**c**) and SCG10 (**d**) expression in neuronal differentiation with kinetin treated neural crest cells derived from FD-iPSC. Results of wound healing assay (**e**) and paxillin staining (**f**) of kinetin treated FD-iPSC derived neural crest cells. $n = 3 - 5$; ***, $P < 0.001$. All values are mean ± s. d.

Supplementary Figure 10: **Five-day treatment of kinetin for FD-iPSC derived neural crest cells. a**, Quantification of Tuj1 expressing neural crest cells derived from FD-iPSC with/without kinetin treatment and Control-iPSC. **b,** MASH1 and SCG10 expression in kinetin-treated neural crest cells derived from FD-iPSC (***, $P < 0.001$). $n = 4 - 6$; All values are mean ± s. d.

Supplementary Figure 11: **Schematic illustration of kinetin treatment regimens**. FD-iPSCs were treated either continuously (28 days) starting 1 day prior to differentiation until analysis (arrowhead) or treated short-term at the neural crest precursor stage following isolation of HNK1+ cells (1 day or 5 day treatment).

Supplementary Table 1: Genetic analysis confirms the identity of FD-fibroblast and FD-iPSC. DNA microsatellite genotyping of FD-fibroblast showed same result as that of FD-iPSC.

Supplementary Table 2: Gene expression array data of significantly up-regulated and down-regulated genes in FD-iPSC derived neural crest cells over H9 embryonic stem cells and C14-iPSC derived counterpart cells.

Supplementary Table 3: Sequences of primers used for sequencing and PCR analysis.